Title: The role of feedback from the auditory cortex in shaping responses to sounds in inferior colliculus.

Authors: Jennifer M. Blackwell[1], Winnie Rao[1], Mariella De Biasi[2,3,4], Maria N. Geffen[1,4,5*]

Affiliation: [1]*Department of Otorhinolaryngology, University of Pennsylvania, Philadelphia, PA*
[2]*Department of Psychiatry, University of Pennsylvania, Philadelphia, PA*
[3]*Department of Systems Pharmacology and Experimental Therapeutics, University of Pennsylvania, Philadelphia, PA*
[4]*Department of Neuroscience, University of Pennsylvania, Philadelphia, PA*
[5]*Department of Neurology, University of Pennsylvania, Philadelphia, PA*

**** Corresponding Author:***
Maria N. Geffen, Ph.D.
Associate Professor
Department of Otorhinolaryngology
Department of Neuroscience
Department of Neurology
University of Pennsylvania
5 Ravdin, 3400 Spruce St.
Philadelphia PA 19104
(215) 898-0782
mgeffen@pennmedicine.upenn.edu
http://www.med.upenn.edu/hearing

Abstract

The extensive feedback from the auditory cortex (AC) to the inferior colliculus (IC) supports critical aspects of auditory learning, but has not been extensively characterized. Furthermore, it remains unknown whether and how intra-cortical processing of auditory information propagates to earlier stages in the auditory pathway. Previous studies demonstrated that responses of neurons in IC are altered by focal electrical stimulation and pharmacological inactivation of auditory cortex, but these methods lack the ability to selectively manipulate the activity of projection neurons. Combining viral technology with electrophysiological recordings, we measured the effects of selective optogenetic activation or suppression of cortico-collicular feedback projections on IC responses to sounds. Activation of cortico-collicular feedback generally increased spontaneous activity and decreased stimulus selectivity in IC, whereas suppression of the feedback did not affect collicular activity. To further understand how microcircuits in the auditory cortex may control collicular activity, we tested the effects of optogenetically modulating different cortical neuronal subtypes, specifically parvalbumin-positive (PV) and somatostatin-positive (SOM) inhibitory interneurons. We found that, despite strong effects on sound-evoked responses across the layers of AC, activating either type of interneuron did not affect IC sound-evoked activity. However, suppression of SOMs, but not PVs, weakly increased spontaneous activity in IC. These findings suggest that shaping of sound responses mediated by cortical inhibition does not affect sound processing in IC. Combined, our results identify that activation of excitatory projections, but not inhibitory-driven increases in cortical activity, affects collicular sound responses.

Significance Statement

Descending projections from the auditory cortex to the auditory midbrain, the inferior colliculus, have been shown to play a critical role in auditory learning and behavior. However, little is known about the details of how this direct feedback shapes neuronal responses to sounds in the inferior colliculus. We found that direct activation of cortico-collicular feedback increased spontaneous and modulated sound-evoked activity in the inferior colliculus. Interestingly, modulation of inhibitory interneuron activity, thereby increasing or decreasing excitatory neuronal activity in the auditory cortex, did not affect sound responses in the inferior colliculus. This work offers evidence that auditory cortex shapes sound responses in the inferior colliculus via direct feedback independently of the activity of cortical inhibitory interneurons.

Introduction

Information processing is typically studied as a set of computations ascending along a hierarchy of sensory areas, often overlooking the role of descending feedback between these nuclei. In the auditory system, the auditory cortex (AC) sends extensive feedback to nuclei earlier in the auditory pathway, including the auditory thalamus (Winer et al., 2001; Alitto and Usrey, 2003; Rouiller and Durif, 2004) and the inferior colliculus (IC) (Saldaña et al., 1996; Winer et al., 1998; Doucet et al., 2003; Bajo and Moore, 2005; Coomes et al., 2005; Bajo et al., 2006). The mechanisms by which information processing is shaped via the *descending feedback* pathway remain poorly characterized. In this study, we selectively modulated activity in AC, targeting either excitatory projections or inhibitory interneurons, to quantify how AC shapes spontaneous activity and sound-evoked responses in IC.

Previous studies demonstrated that neuronal responses to sounds in IC are altered by focal electrical stimulation and inactivation of AC. Cortical stimulation shifted tuning properties of IC neurons toward those of the stimulated neurons in frequency (Jen et al., 1998; Yan and Suga, 1998; Ma and Suga, 2001a; Jen and Zhou, 2003; Yan et al., 2005; Zhou and Jen, 2007), amplitude (Jen and Zhou, 2003; Yan et al., 2005; Zhou and Jen, 2007), azimuth (Zhou and Jen, 2005, 2007), and duration (Ma and Suga, 2001b). Stimulation of AC had mixed effects on sound-evoked responses in IC, increasing and decreasing responses in different subpopulations of neurons (Jen et al., 1998; Zhou and Jen, 2005). Consistent with this effect, different patterns of direct cortico-collicular activation enhanced or suppressed white noise-induced responses in IC (Vila et al., 2019). AC inactivation studies, on the other hand, found less consistent effects on IC responses. Whereas pharmacological inactivation of AC caused a shift in best frequency in IC neurons (Zhang et al., 1997), several studies show inactivation of AC had no effect on frequency selectivity in IC (Jen et al., 1998), but rather modulated sound-evoked and spontaneous activity (Gao and Suga, 1998; Popelář et al., 2003, 2016). Cortico-collicular feedback is critical to auditory learning, specifically learning to adapt to a unilateral earplug during sound localization (Bajo et al., 2009). Pairing electrical leg stimulation with a tone induced a shift in best frequency of IC neurons, while presentation of a tone alone was insufficient (Gao and Suga, 1998, 2000). Furthermore, cortico-collicular feedback was necessary to induce running in response to a loud noise (Xiong et al., 2015).

In AC, interactions between excitation and inhibition shape sound responses in excitatory cell populations. Modulating activity of different inhibitory interneuron subtypes in AC narrowed frequency tuning and attenuated tone-evoked responses of excitatory neurons, while suppression had the opposite effect (Hamilton et al., 2013; Aizenberg et al., 2015; Seybold et al., 2015; Phillips and Hasenstaub, 2016). Electrical stimulation of AC, cooling or pharmacological inactivation affected the amplitude of sound-evoked responses and shifted the best frequency of neurons in IC, but it remains unknown how specific these effects are to direct feedback, and whether the effects of intra-cortical inhibition propagate to the IC.

The goal of the present study is to examine the role of cortico-collicular projections in shaping sound responses in IC. IC receives glutamatergic (Feliciano and Potashner, 1995) inputs from neurons originating predominantly in layer 5 of AC (Saldaña et al., 1996; Winer et al., 1998; Doucet et al., 2003; Bajo and Moore,

2005; Coomes et al., 2005; Bajo et al., 2006). We used viral transfection methods to selectively drive excitatory or inhibitory opsin expression in AC-IC projections. We then recorded neuronal activity in IC and tested how activation or suppression of AC-IC projections affected spontaneous activity and sound-evoked responses in IC. To better understand whether and how intra-cortical network interactions propagated to IC, we manipulated the activity of the two most common inhibitory neuronal subtypes in AC, Parvalbumin-(PV) and Somatostatin-(SOM) positive interneurons (Rudy et al., 2011).

Materials and Methods

Animals.

All experiments were performed in adult male and female mice (supplier: Jackson Laboratories; age, 12–15 wk; weight, 22–32 g; PV-Cre mice, strain: B6; 129P2-Pvalbtm1(cre)Arbr/J; SOM-Cre mice, strain: Ssttm2.1(cre)Zjh/J; Cdh23 mice, strain: Cdh23tm2.1Kjn/J, or PV-Cre x Cdh23 or SOM-Cre x Cdh23 crosses). Mice were housed at 28°C on a 12 h light–dark cycle with water and food provided ad libitum, less than five animals per cage. In PV-Cre mice Cre recombinase (Cre) was expressed in parvalbumin-positive interneurons, and in SOM-Cre, Cre was expressed in somatostatin-positive interneurons. All animal work was conducted according to the guidelines of University of Pennsylvanian IACUC and the AALAC Guide on Animal Research. Anesthesia by isofluorane and euthanasia by ketamine were used. All means were taken to minimize the pain or discomfort of the animals during and following the experiments. All experiments were performed during the animals' dark cycle.

Viral Vectors.

Modified AAVs encoding ArchT (AAV9-CAG-FLEX-ArchT-GFP or AAV9-CAG-FLEX-ArchT-tdTomato; UNC Vector Core) or ChR2 (AAV9-CAG-FLEX-ChR2-tdTomato; Penn Vector Core) were used for selective suppression or excitation, respectively. Retrograde AAV virus encoding Cre (retro AAV-hSyn-Cre-GFP) was custom made in our laboratory. Briefly, RetroAAV2 hSyn Cre-GFP was packaged using the Helper-Free system (Agilent) and the retrograde trafficking plasmid, Retro2, which bears capsid mutations in serotype 2.

Surgery and Virus Injection.

At least 21 days prior to electrophysiological recordings, mice were anesthetized with isoflurane to a surgical plane. The head was secured in a stereotactic holder. The mouse was subjected to a small craniotomy (2 x 2 mm) over AC under aseptic conditions. Viral particles were injected (750 nl) bilaterally using a syringe pump (Pump 11 Elite, Harvard Apparatus) targeted to AC (coordinates relative to bregma: −2.6 mm anterior, ±4.3 mm lateral, +1 mm ventral). Fiber-optic cannulas (Thorlabs, Ø200 µm Core, 0.22 NA) were implanted bilaterally over the injection site at depth of 0.5 mm from the scull surface. For a subset of mice, to target direct feedback, the mouse was also subjected to a craniotomy over IC (1 x 4 mm). Retro AAV viral construct was injected (3 x

200 nl) via glass syringe (30-50 um diameter) using a syringe pump (Pump 11 Elite, Harvard Apparatus) bilaterally in IC. Craniotomies were covered with a removable silicon plug. A small headpost was secured to the skull with dental cement (C&B Metabond) and acrylic (Lang Dental). For postoperative analgesia, slow release Buprenex (0.1 mg/kg) and Bupivicane (2 mg/kg) were injected subcutaneously. An antibiotic (5 mg/kg Baytril) was injected subcutaneously daily (for 4 days) at the surgical site during recovery. Virus spread was confirmed postmortem by visualization of the fluorescent protein expression in fixed brain tissue, and its colocalization with PV or SOM, following immuno-histochemical processing with the appropriate antibody.

Acoustic Stimuli.

Stimuli were delivered via a magnetic speaker (Tucker-David Technologies) directed toward the mouse's head. Speakers were calibrated prior to the experiments to ±3 dB over frequencies between 3 and 70 kHz by placing a microphone (Brüel and Kjaer) in the location of the ear contralateral to the recorded AC hemisphere, recording speaker output and filtering stimuli to compensate for acoustic aberrations (Carruthers et al., 2013).

Tuning Stimuli. (1) To measure tuning for direct feedback cohorts, a train of 50 pure tones of frequencies spaced logarithmically between 3 and 70 kHz, at 70 dB sound pressure level relative to 10 microPascals (SPL) relative to 20 μPa, in pseudo-random order was presented 20 times. Each tone was 50 ms duration (5-ms cosine squared ramp up and down) with an inter-stimulus interval (ISI) of 450 ms. Alternating tones were paired with continuous 250 ms laser pulse at either -100 ms, -20 ms, or +8 ms onset relative to tone onset.

(2) For SOM-Cre and PV-Cre cohorts, a train of pure tones of 35 frequencies spaced logarithmically between 3 and 70 kHz and 8 uniformly spaced intensities from 0 to 70 dB SPL were presented 10 times in a pseudo-random order. Alternating tones were paired with continuous 250 ms laser pulse at -100 ms relative to tone onset.

Dynamic Random Chords (DRCs). To measure spectro-temporal receptive fields (STRFs) we constructed DRCs from 20 ms chords (with 1 ms ramp) of 50 frequencies spaced logarithmically between 5 and 40 kHz with average intensity of 50 dB SPL and 20 dB SPL standard deviation. Total duration was 40 minutes with a 250 ms continuous laser pulse presented every 1 s.

Electrophysiological Recordings.

All recordings were carried out inside a double-walled acoustic isolation booth (Industrial Acoustics). Mice were placed in the recording chamber, and a headpost was secured to a custom base, immobilizing the head. Activity of neurons in AC were recorded via a custom silicon multi-channel probe (Neuronexus), lowered in the area targeting AC via a stereotactic instrument following a craniotomy at a 35-degree angle. The electrode tips were arranged in a vertical fashion that permits recording the activity of neurons across the depth of the auditory cortex and the inferior colliculus. Activity of neurons in IC were recorded via the same custom probes, lowered in the area targeting IC via a stereotactic instrument following either a craniotomy (SOM-Cre and PV-Cre

cohorts) or removal of the silicon plug, vertically. Electro-physiological data from 32 channels were filtered between 600 and 6000 Hz (spike responses), digitized at 32kHz and stored for offline analysis (Neuralynx). Spikes belonging to single neurons and multi-units were detected using commercial software (Plexon). We examined the following experimental conditions: Cdh23 + ArchT (N = 4 male mice, awake) Cdh23 + ChR2 (N = 5 male mice, awake) SOM-Cre + ChR2 (N = 15 male mice; 8 anesthetized, 7 awake) SOM-Cre + ArchT (N = 7 mice; 4 female, 3 male, 4 anesthetized, 3 awake) PV-Cre + ChR2 (N = 16 male mice; 12 anesthetized, 4 awake) PV-Cre + ArchT (N = 4 male mice, awake). For cohorts with awake and anesthetized recordings data were analyzed separately, but we observed no difference in our results so data were combined. Mice that did not show effect of laser activation or suppression in auditory cortex were excluded.

Photostimulation of Neuronal Activity.

Neurons were stimulated by application of continuous light pulse delivered from either blue (473 nm, BL473T3-150, used for ChR2 stimulation) or green DPSS laser (532 nm, GL532T3-300, Slocs lasers, used for ArchT stimulation) through implanted cannulas. Timing of the light pulse was controlled with microsecond precision via a custom control shutter system, synchronized to the acoustic stimulus delivery.

Neural Response Analysis.

Unit selection. Units were selected based on pure-tone responsiveness. For each unit we identified the 7 frequencies that elicited the highest response and averaged activity across these trials (and the highest 3 amplitudes for stimulus with multiple amplitudes). Units with tone-evoked activity (75 ms window after tone onset) less than two standard deviations above the spontaneous activity (50 ms window prior to tone onset) in no laser condition were excluded from the analysis. Both single units and high quality multi-units were used.

Spontaneous activity and tone-evoked response magnitude. Feedback cohort: Spontaneous activity was the average firing rate in a 20 ms window prior to tone onset of top 7 preferred frequencies.

SOM-Cre/PV-Cre cohorts: Spontaneous activity was the average firing rate in a 50 ms window prior to tone onset of top 7 preferred frequencies and 3 highest amplitudes.

All mice: Tone-evoked response magnitude was calculated as the difference between the average tone-evoked response in a 75 ms window after tone onset and the spontaneous activity.

Sparseness. To examine frequency selectivity of neurons, sparseness of frequency tuning was computed as:

$$Sparseness = 1 - \frac{\left(\sum_{i=1}^{i=n} \frac{FR_i}{n}\right)^2}{\sum_{i=1}^{i=n} \frac{FR_i^2}{n}}$$

where FR_i is tone-evoked response to tone at frequency i, and n is number of frequencies used (Weliky et al., 2003). Subgroups of neurons used in sparseness analyses were separated based on > 1 standard deviation change based on the -100 ms laser onset trials.

Linear fits across frequencies. Linear fits were calculated using linear regression (fitlm.m; MATLAB) over 50 data points, one for each of the 50 frequencies tested (Natan et al., 2017b). The 50 data points were separately calculated as the mean FR over all repeats of each frequency.

Best Frequency. Best frequency was defined as the frequency that elicited the maximum response.

STRF Analysis. To calculate the STRF we separated the stimulus into 1-second chunks, concatenating the 250 ms laser ON chunks and the 250 ms laser OFF chunks immediately preceding laser onset. These data were then used to calculate the average spectrogram preceding a spike. Subsequently we averaged the STRF across the eight stimulus files. To determine the significance of the cluster, the *z*-score of pixels was computed relative to the baseline values from an STRF generated with scrambled spike trains, using Stat4ci toolbox (Chauvin et al., 2005; Natan et al., 2017a). We ran this significance test 100 times and any pixel identified as significant more than 90 times was considered significant. Clusters were matched between laser ON and laser OFF trials by comparing the overlap of the clusters, requiring a 50% overlap of the smallest cluster size to be a match. From STRF, the peak time, temporal width, peak frequency, and frequency width of the positive and negative clusters were measured (Woolley et al., 2006; Shechter and Depireux, 2007; Schneider and Woolley, 2010).

Statistical Analyses.

Significant differences and *P* values were calculated using paired Wilcoxon sign-rank test (unless noted otherwise) with standard MATLAB routine. For the laser alone data, to compare distributions to standard normal distribution data were normalized by mean and standard deviation and then significant differences and *P* values were calculated by Kolmogorov-Smirnoff test with standard MATLAB routine. Mean ± standard error of the mean was reported unless stated otherwise. * indicates $p < 0.05$, ** indicates $p < 0.01$, *** indicates $p < 0.001$.

Results

Activating direct cortico-collicular feedback modulates activity in the inferior colliculus

Our first goal was to characterize the effects of activating the direct cortico-collicular projections on tone-evoked responses in IC. We used a viral transfection strategy to deliver either an excitatory opsin, ChannelRhodopsin2 (ChR2) or an inhibitory opsin, ArchaerhodopsinT (ArchT), bilaterally, specifically to the neurons in the auditory cortex which project to the inferior colliculus. To achieve such specificity, we injected a retrograde virus that encoded Cre recombinase (Retro2 AAV.Cre) in IC. This retrograde viral construct ensured that all neurons projecting to IC expressed Cre recombinase a few weeks later. At the same time, we injected a virus that encoded ChR2 or ArchT in reversed fashion under the FLEX cassette in AC (AAV.Flex.ChR2,

AAV.Flex.ArchT). This strategy ensured that only neurons expressing Cre recombinase in the auditory cortex would express ChR2 or ArchT in AC. Therefore, opsin was expressed exclusively in AC-IC projecting neurons (**Figure 1 A,B**). Shining light over AC of these mice would therefore directly activate or suppress only this cortico-collicular pathway.

First, we measured and quantified neuronal spiking in IC in response to stimulation or suppression of cortico-collicular projections. To activate these neurons, we shone blue laser over AC, recorded neuronal activity in IC, and quantified the effects of manipulating feedback in the absence of sound (**Figure 1 E,F**). We measured the spiking activity as we varied the duration of laser manipulation (1 ms, 5 ms, 25 ms, 250 ms). As expected, activation of cortico-collicular neurons resulted, on average, in an increase in firing rate of IC neurons. This effect persisted at all laser durations we used. Specifically, for all durations the distribution of the change in activity with activation was significantly different from normally distributed around zero (**Figure 1E**; 1 ms: $p = 3.07e-15$, mean = 1.1 stdevs, median = 0.21 stdevs; 5 ms: $p = 4.4e-20$, mean = 1.7 stdevs, median = 0.19 stdevs; 25 ms: $p = 5.5e-17$, mean = 1.6 stdevs, median = -0.021 stdevs; 250 ms: $p = 3.4e-12$, mean = 0.58 stdevs, median = 0.101 stdevs, Kolmogorov-Smirnov test). Whereas the direction of the effect was consistent with our prior expectations, the magnitude of the effect was unexpectedly small. This suggests that AC targets a small subpopulation of IC neurons and that the effect of activation does not spread too far within IC.

We tested the effect of suppressing AC-IC neurons on firing responses in IC and, surprisingly, we detected no difference in firing in IC neurons. For all laser durations the population of responses were normally distributed around zero change in activity (**Figure 1F**). This result suggests that AC-IC inputs at rest do not contribute to IC responses, but rather modulate collicular activity only when activated.

Next, our goal was to characterize modulation of sound-evoked responses in IC by cortical feedback. We first tested the effects of feedback modulation on acoustic click responses. We chose clicks as the initial stimulus because they drive fast responses in both AC and IC. Laser stimulation began 100 ms prior to click train onset to allow for the response to the laser to come to a steady state, and continued activation throughout the clicks. Activating the feedback had a weak suppressive effect on the firing rate of IC neurons in response to clicks. Consistent with previous experiments, we observed an overall increase in spontaneous activity (**Figure 1E**, bottom; $p = 0.0031$, spont ON = 5 ± 0.87 Hz, spont OFF = 4.3 ± 0.92 Hz). Activating feedback caused a small decrease in click-evoked response (**Figure 1G**, left; $p = 0.001$, click ON = 10.4 ± 1.2 Hz, click OFF = 10.7 ± 1.1 Hz).

By contrast, suppressing cortico-collicular feedback using ArchT had no effect on IC click responses (**Figure 1H**). Because attenuating the input does not affect the activity in IC during clicks this result further suggests that the strength of the baseline signal from AC to IC, even in the presence of cortical activity, is not sufficient to modulate IC responses.

We also tested whether the effects of cortico-collicular modulation differed across the receptive field of collicular neurons. We presented a stimulus that consisted of tones of 50 frequencies ranging from 3 to 70 kHz.

To modulate the feedback from AC, we tested three different laser onsets (-100 ms, -20 ms, +8 ms) relative to tone onset to isolate the effect of timing on affecting IC responses. These delays were chosen for the following reasons: -100ms delay would allow for the laser effect on cortical activity to come to a steady state, making it easier to quantify the effect throughout the tone pip; +8 ms is set up to mimic the time scale of cortical response to a tone, effectively amplifying the onset of the cortical response; -20 ms delay is an intermediate value.

We found that whereas activating feedback increased spontaneous activity of IC neurons (**Figure 2A**, left; -100 ms: p = 0.022, ON = 4.3 ± 0.47 Hz; OFF = 3.6 ± 0.38; -20 ms: p = 8.6e-6, ON = 5.6 ± 0.63, OFF = 3.7 ± 0.47), overall the feedback decreased tone-evoked response magnitude in IC, which we defined as the difference between spontaneous and tone-evoked response, at all laser onsets (**Figure 2A**, right; -100 ms: p = 3.2e-5, ON = 14.2 ± 0.98 Hz; OFF = 15.5 ± 1.04 Hz; -20 ms: p = 1.4e-6, ON = 11.8 ± 1.08 Hz, OFF = 13.9 ± 1 Hz; +8 ms: p = 0.0034, ON = 13.03 ± 1.03, OFF = 13.7 ± 1.03). This suggests that the broad activation of feedback upregulates the baseline activity of IC neurons, but decreases tone-evoked response (**Figure 3E**). By contrast, suppressing the feedback had no effect on either spontaneous activity or tone-evoked response magnitude (**Figure 2B**), suggesting that at baseline, AC does not provide strong modulation of IC activity, as removing it does not affect sound-evoked effects in IC.

We then examined the effect of feedback on frequency tuning of IC units. Activation of feedback decreased frequency selectivity in the subsets of units that also showed a decrease in tone-evoked response magnitude or increase in spontaneous activity, but not in units that showed an increase in tone-evoked response magnitude or decrease in spontaneous activity (**Figure 3A**, mag decrease: -20 ms, p = 0.00031, sparse ON = 0.49 ± 0.027, sparse OFF = 0.55 ± 0.025; +8 ms, p = 0.00029, sparse ON = 0.46 ± 0.027, sparse OFF = 0.55 ± 0.024; spont increase: -100 ms, p = 0.011, sparse ON = 0.49 ± 0.032, sparse OFF = 0.56 ± 0.031; -20 ms, p = 0.00018, sparse ON = 0.46 ± 0.034, sparse OFF = 0.56 ± 0.029; +8 ms, p = 2.2e-6, sparse ON = 0.41 ± 0.032, sparse OFF = 0.55 ± 0.029). Over the population of neurons with decreased tone-evoked response magnitude and/or increased spontaneous activity, the median slopes and y-intercepts of ranked linear fits to frequency responses are less than 1 and above zero, respectively (**Figure 3D**). These results, in combination with the decreased tone-evoked activity observed (**Figure 3E**, *-100ms*: p = 0.018, ON = 19.01 ± 1.2 Hz, OFF = 18.5 ± 1.2 Hz; *+8ms*: p = 0.007, ON = 17.3 ± 1.2 Hz; OFF = 16.9 ± 1.2 Hz), indicate the decrease in frequency selectivity was due to a decrease in response to tones at preferred frequencies, not non-preferred frequencies. This result suggests that the suppressive effect of the feedback is preferential for higher firing responses. Suppressing feedback resulted in very small (< 0.04 %) change in sparseness, therefore it did not affect frequency selectivity (**Figure 3B**).

To better understand the effect of modulation of cortical activity on spectro-temporal receptive field properties of IC neurons, we presented a continuous signal comprised of dynamic random chords (DRCs) sampled from a uniform distribution of loudness values per frequency bin. The unbiased nature of this stimulus allowed us to estimate the spectro-temporal receptive field of neurons (STRF), which quantifies the dynamics of sound waveform in time and frequency that lead to a neuronal response. During the DRC stimulus, we turned on the

laser every other second for 250 ms to either activate or suppress cortico-collicular projections. We found that a subset of cells reduced their mean DRC-evoked firing rates (N = 56), whereas another subset of cells increased their mean DRC-evoked firing rate when we activated cortico-collicular feedback (N = 47). We next separately computed the receptive fields for each neuron when laser was off and when laser was on and compared the STRFs. To quantify those changes, we identified the positive (activation) and negative (suppressive) regions in the STRFs and compared them for laser ON and laser OFF conditions. In the subset of neurons whose firing rate increased with laser STRFs changed: only 42% of positive lobes, and 63% of negative lobes persisted with the laser (**Figure 4B**, left). Of those lobes that persisted, for positive lobes, there was on average a decrease in temporal width (p = 0.00098, ON = 0.0303 ± 0.0018 s, OFF = 0.037 ± 0.0023 s), frequency selectivity (p = 0.00042, ON = 6.7 ± 1.1 Hz, OFF = 9.6 ± 1.8 Hz) and STRF size (p = 0.00036, ON = 46.05 ± 6.9 pixels, OFF = 77.5 ± 12.04 pixels), whereas for negative lobes, we did not detect any changes (**Figure 4C**, left). In neurons whose firing rate was decreased, there was a much smaller change in the lobes, with 78% and 79% of positive and negative lobes persisting, respectively (**Figure 4B**, right). For both positive lobes and negative lobes, the only difference was an increase in the temporal width when laser was activated (**Figure 4C**, right; Positive lobes: p = 0.026, ON = 0.034 ±0.0025 s, OFF = 0.032 ± 0.0025 s; Negative lobes: p = 0.02, ON = 0.037 ± 0.0028 s, OFF = 0.032 ± 0.0024 s). The decrease in STRF size in units with increased DRC-evoked response and decrease in sparseness across the population is consistent with the interpretation that the effect of the feedback leads to a decrease in responsiveness to tones that evoke the greatest responses (in the center of the receptive field) and an increase to stimuli that evoke weaker activity. In other words, neuronal firing increases overall, but selective responses to specific frequency bands decrease.

Modulating inhibitory neuronal activity in AC does not affect collicular sound responses

Auditory responses in AC are shaped by interactions between excitatory and inhibitory neurons (Wood et al., 2017). To determine how modulating frequency selectivity in AC might affect tone-evoked responses in IC in a frequency-selective fashion, we perturbed the excitatory-inhibitory interactions by modulating two different classes of inhibitory interneuron known to contribute to sound responses in AC: PV and SOM inhibitory interneurons. We found that modulating PV interneuron activity in AC had little effect on spontaneous and tone-evoked activity or frequency selectivity in IC (**Figure 5 B-E**) despite modulating frequency selectivity, spontaneous activity, and tone-evoked response magnitude in AC. Specifically, in AC, activating PVs decreased spontaneous activity and tone-evoked response magnitude (**Figure 5F**; spontaneous activity: p = 2.2e-9, ON = 0.88 ± 0.16 Hz, OFF = 2.7 ± 0.34 Hz; tone-evoked response magnitude: p = 8.02e-7, ON = 6.9 ± 1.06 Hz, OFF = 11.5 ± 1.3 Hz**)** and increased frequency selectivity (**Figure 5G**; p = 3.3e-12, ON = 0.59 ± 0.022, OFF = 0.42 ± 0.02), while suppressing PVs increased spontaneous activity (**Figure 5I**; p = 5.2e-5, ON = 4.08 ± 0.54 Hz, OFF = 3.06 ± 0.55 Hz) and decreased frequency selectivity (**Figure 5J**; p = 3.8e-5, ON = 0.34 ± 0.027, OFF = 0.41 ±

0.031). This suggests that the increase in cortical activity driven by broad PV activation does not propagate to the inferior colliculus.

Different interneuron classes may function in distinct networks, so we also tested the effects of modulating SOM interneurons. Modulating SOM interneurons had no effect on tone-evoked activity (**Figure 6 B,D**, right) or frequency selectivity (**Figure 6 C,E**), but suppressing SOM interneurons increased spontaneous activity in IC (**Figure 6D**, left; p = 0.029, ON = 6.9 ± 0.66 Hz, OFF = 6.7 ± 0.63 Hz), a change that we also observed with activation of the direct feedback projections (**Figure 2A**, left). Similar to PV interneurons, activating SOM interneurons decreased spontaneous activity and tone-evoked response magnitude in AC (**Figure 6F**; spontaneous activity: p = 1.4e-12, ON = 0.97 ± 0.25 Hz, OFF = 2.9 ± 0.37 Hz; tone-evoked response magnitude: p = 1.3e-15, ON = 3.3 ± 0.59 Hz, OFF = 11.4 ± 1.2 Hz) and increased frequency selectivity (**Figure 6G**; p = 1.6e-13, ON = 0.69 ± 0.024, OFF = 0.47 ± 0.019). In AC, suppressing SOMs reduced spontaneous activity, but had no significant effect on tone-evoked response magnitude or frequency selectivity (**Figure 6 I,J**; p = 8.1e-4, ON = 3.6 ± 0.41 Hz, OFF = 2.2 ± 0.38 Hz). This lack of effect was not due to the relatively small effect of light penetrating to the deep layers. In fact, to confirm that modulating PV and SOM activity in AC affected activity of units in L5/6 where the feedback projections we looked at changes in spontaneous activity at each tetrode which spanned the entire auditory cortex. We found that activity was modulated across the layers (**Figure 5-6 H,K**). Whereas modulating PVs did not have an effect on IC activity, SOM suppression resulted in an increase in spontaneous, but not tone-evoked activity in IC, which suggests that inhibitory modulation of sound responses in AC does not propagate to IC.

Discussion

Auditory cortex sends extensive projections to IC (Saldaña et al., 1996; Winer et al., 1998; Doucet et al., 2003; Bajo and Moore, 2005; Coomes et al., 2005; Bajo et al., 2006). Our results demonstrate that activation of this cortico-collicular feedback modulates sound responses in IC by upregulating spontaneous IC activity, but decreasing frequency selectivity and reducing spectro-temporal receptive field size in IC. Interestingly, suppressing cortico-collicular feedback had little effect on IC activity, which suggests that at baseline and during passive tone presentation the feedback does not affect activity of IC neurons. We also found that SOM, but not PV inhibitory interneurons modulated IC activity, suggesting that the effects of modulation of cortical activity by PVs does not back-propagate to IC, whereas SOM-driven modulation affects spontaneous activity, but not tone-evoked responses. Overall our findings imply that direct cortico-collicular feedback can modulate responses to simple (pure tones) and more complex (DRCs) auditory stimuli by reducing, rather than increasing, sound selectivity. This modulation occurs independently of the activity of cortical inhibitory interneurons.

Whereas optogenetic manipulation allows for temporally precise control and cell-type specificity, the technique lacks the spatial specificity of electrical stimulation. Since both AC and cortico-collicular projections are tonotopically organized (Lim and Anderson, 2007; Markovitz et al., 2013; Barnstedt et al., 2015; Straka et al.,

2015), spatially specific stimulation can more accurately mimic frequency-specific responses by activating specific regions in the tonotopic map. Previous studies found that electrical stimulation of AC caused best frequencies in IC to shift towards the best frequencies of the stimulated site in AC (Gao and Suga, 1998, 2000; Yan and Suga, 1998; Ma and Suga, 2001a; Yan et al., 2005; Zhou and Jen, 2007). These results suggest that cortico-collicular feedback may be important for increasing the representation of behaviorally relevant stimuli in IC. However, when activating direct feedback, we did not observe consistent changes in IC best frequencies (**Figure 3F**). In this activation paradigm, we activated feedback projections across cortex, and therefore across the tonotopic map, so it is unsurprising that we did not find shifts in the best frequencies of neurons.

Previous studies found no effect of activating projection terminals on responses in the central nucleus of IC, only shell regions of IC (Xiong et al., 2015), which are the predominant targets of cortico-collicular feedback. In our study we were able to record from a larger neuronal population, revealing a subset of neurons in central IC that were modulated by feedback. This is consistent with another study which observed enhanced white noise-induced activity in a small subset of neurons in the central nucleus of IC with activation of direct cortico-collicular feedback (Vila et al., 2019). The effects in central IC may be due to direct cortico-collicular feedback, intra-collicular circuits (Saldaña and Merchań, 1992; Malmierca et al., 1995; Miller et al., 2005; Sturm et al., 2014) , or a combination of these mechanisms.

Inactivation studies have shown mixed effects on sound-evoked responses in IC, but consistently demonstrated no effect on frequency selectivity. Specifically, suppression of AC increased or decreased IC sound responses in distinct subsets of cells (Popelář et al., 2003, 2016) while suppression of direct cortico-collicular feedback terminals in IC decreased sound-evoked responses (Xiong et al., 2015). However, our results show that suppression of direct cortico-collicular feedback has inconsistent effects on frequency selectivity and no effect on any other sound response properties in IC. Xiong et al. found changes in IC responses specifically in the shell regions of IC, while our study targeted the central nucleus of IC, thus it is plausible that the difference in the recording locations might explain this discrepancy.

Our interest in central IC is due to its frequency tuning properties and that it is part of the behavioral output pathway leading to the pedunculopontine tegmental nucleus, which controls pre-pulse inhibition (PPI) of the acoustic startle reflex. Understanding how AC modulates sound responses in central IC may provide insight into how AC drives changes in auditory behaviors. Previously, we found that behavioral frequency discrimination acuity changed after differential auditory fear conditioning and these changes were driven by the auditory cortex (Aizenberg and Geffen, 2013; Aizenberg et al., 2015). The behavioral task used to test frequency discrimination acuity was a modified PPI task. Although AC can modulate this behavior, PPI is still observed after decerebration (Li and Frost, 2000) and the underlying circuit is believed to be subcortical (Fendt et al., 2001). The IC is a critical structure in the PPI circuit (Leitner and Cohen, 1985; Li et al., 1998; Fendt et al., 2001), with the central nucleus of IC receiving ascending auditory projections and the external nucleus of IC acting as the output station (Fendt et al., 2001; Li and Yue, 2002). The broad frequency tuning in the shell regions of the IC (Syka et al., 2000;

Barnstedt et al., 2015) made the central nucleus of IC, which has sharper tuning and a tonotopic organization (Syka et al., 2000; Ehret et al., 2003; Malmierca et al., 2008; Barnstedt et al., 2015), a good candidate for how AC may drive changes in frequency discrimination acuity. Limited evidence for a descending pathway from AC to the pedunculopontine tegmental nucleus (Schofield and Motts, 2009) suggests another alternative pathway by which AC modulates frequency discrimination.

One caveat of our study is that our experiments were performed in passively listening mice. It is possible that the lack of effect we observe with suppression of cortico-collicular feedback is due to the lack of task engagement. Previous studies have found that inactivation of this pathway affects innate responses to sound (Xiong et al., 2015) and auditory learning (Bajo et al., 2009). Furthermore, studies have found that task engagement modulates neuronal responses to sounds (Fritz et al., 2003; Lakatos et al., 2013; McGinley et al., 2015; Downer et al., 2017). Thus, we would expect suppression of this pathway to affect sound processing in IC during a behavioral task. Future studies should explore how activity changes with an animal actively engaged in a behavioral task.

Acknowledgements. This work was supported by National Institutes of Health (Grant numbers NIH R03DC013660, NIH R01DC014700, NIH R01DC015527), Klingenstein Award in Neuroscience, Human Frontier in Science Foundation Young Investigator Award and the Pennsylvania Lions Club Hearing Research Fellowship to MGN. MNG is the recipient of the Burroughs Wellcome Award at the Scientific Interface. JMB was supported by NIH T32MH017168. We thank the members of the Geffen laboratory and the Hearing Research Center at the University of Pennsylvania, including Dr. Steve Eliades and Dr. Yale Cohen for comments on an earlier version of the manuscript. We also thank Sarah Kwon for assistance with confocal imaging.

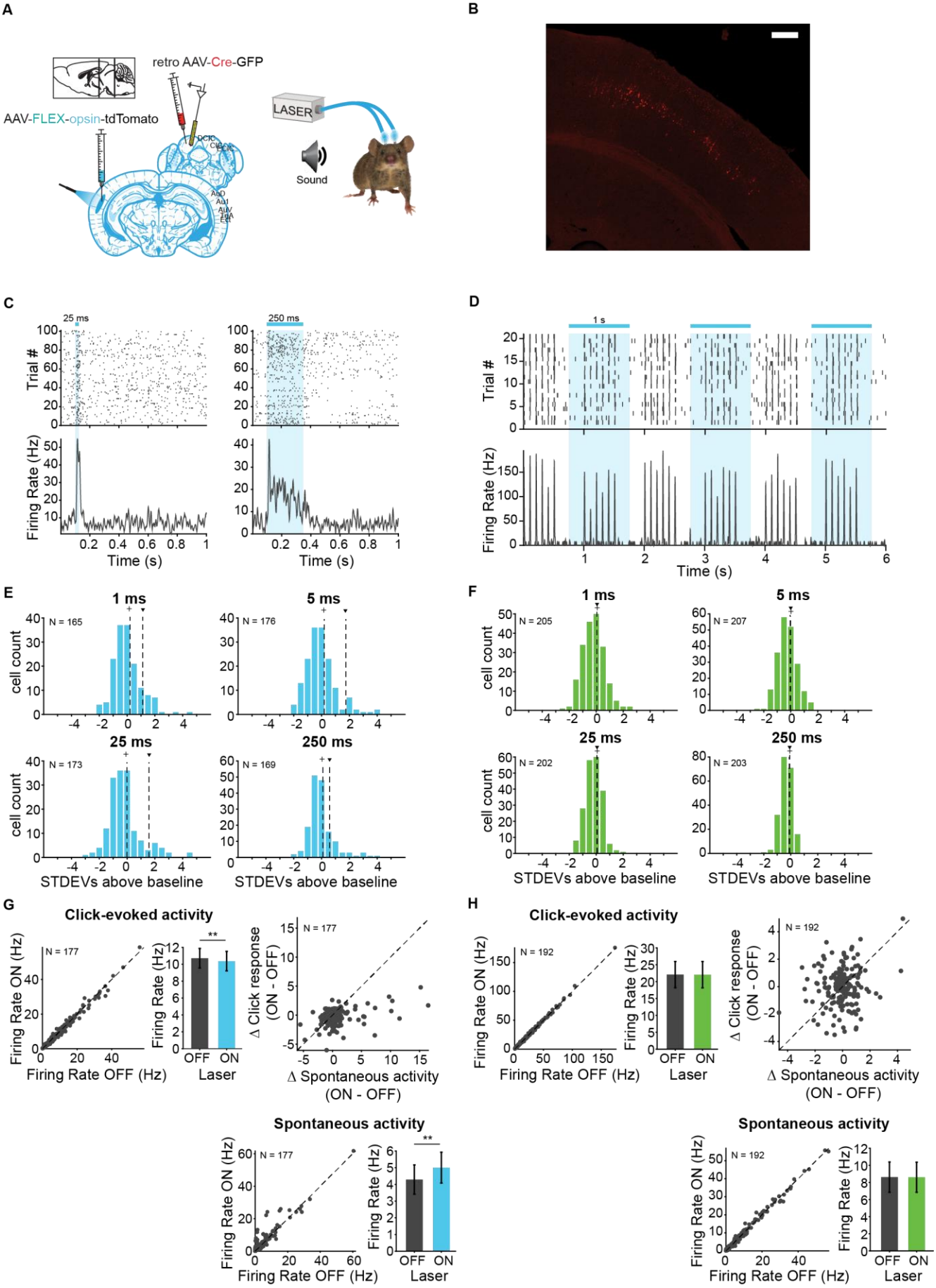
A
retro AAV-Cre-GFP
AAV-FLEX-opsin-tdTomato
LASER
Sound
B
C
25 ms
250 ms
Trial #
Firing Rate (Hz)
Time (s)
D
1 s
Trial #
Firing Rate (Hz)
Time (s)
E
1 ms
5 ms
25 ms
250 ms
N = 165
N = 176
N = 173
N = 169
cell count
STDEVs above baseline
F
1 ms
5 ms
25 ms
250 ms
N = 205
N = 207
N = 202
N = 203
cell count
STDEVs above baseline
G
Click-evoked activity
N = 177
Firing Rate ON (Hz)
Firing Rate OFF (Hz)
Firing Rate (Hz)
OFF
ON
Laser
Δ Click response (ON - OFF)
Δ Spontaneous activity (ON - OFF)
Spontaneous activity
H
Click-evoked activity
N = 192
Spontaneous activity

Figure 1. Effects of modulating feedback activity on responses in IC in the absence of sounds and to clicks. **A** Experimental design: Injection of retro AAV.Cre into IC and anterograde AAV.Flex.opsin into AC and record from IC (left) in awake mice while shining laser into AC, all performed bilaterally (right). **B** Image of opsin-tdTomato expression in cortico-collicular feedback projections in AC. Scale bar: 200um. **C** Example unit response to two laser pulse durations (blue), 25 ms (left) and 250 ms (right). **D** Example unit response to clicks with (blue) and without laser. **E** Distributions of change in unit activity in response to different laser durations in ChR2 cohort (1 ms, 5 ms, 25 ms, 250 ms), + indicates median, ▼ indicates mean. These distributions are not normally distributed (Kolmogorov-Smirnov test; *1 ms*: p = 3.07e-15, mean = 1.1 stdevs, median = 0.21 stdevs; *5 ms*: p = 4.4e-20, mean = 1.7 stdevs, median = 0.19 stdevs; *25 ms*: p = 5.5e-17, mean = 1.6 stdevs, median = -0.021 stdevs; *250 ms*: p = 3.4e-12, mean = 0.58 stdevs, median = 0.101 stdevs). **F** Distributions of change in unit activity in response to different laser durations in ArchT cohort (1 ms, 5 ms, 25 ms, 250 ms), + indicates median, ▼ indicates mean. These distributions are normally distributed (Kolmogorov-Smirnov test). **G** Population response to clicks with activation shows a decrease in click response (left; p = 0.001, click ON = 10.4 ± 1.2 Hz, click OFF = 10.7 ± 1.1 Hz) and an increase in spontaneous activity (bottom; p = 0.0031, spont ON = 5 ± 0.87 Hz, spont OFF = 4.3 ± 0.92 Hz). **H** Population response to clicks with suppression shows no change in activity.

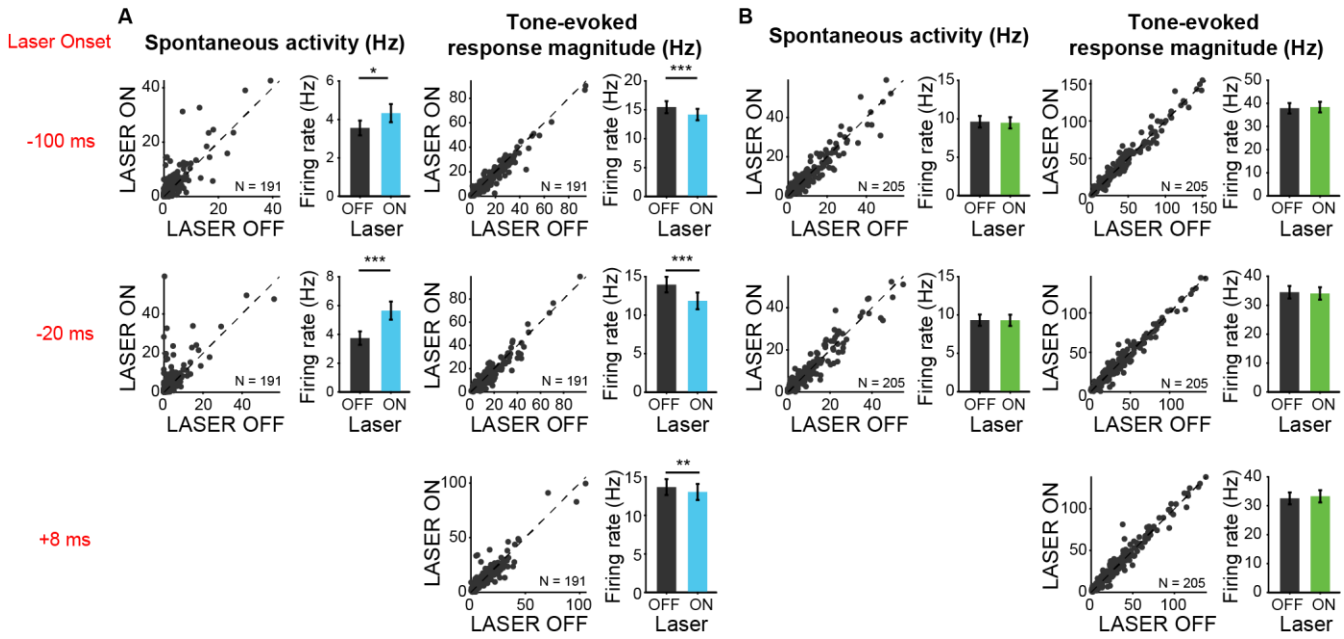

Figure 2. Effects of modulating feedback activity on spontaneous and tone-evoked response magnitude in IC. Left panels: neuronal activity (spontaneous, left or tone-evoked, right) on laser on versus laser off trials. Right panels: Average neuronal activity (spontaneous, left or tone-evoked, right) for laser on and laser off trials. **A** Activating feedback increased spontaneous activity (left; *-100 ms*: p = 0.022, ON = 4.3 ± 0.47 Hz; OFF = 3.6 ± 0.38; *-20 ms*: p = 8.6e-6, ON = 5.6 ± 0.63, OFF = 3.7 ± 0.47) and decreased tone-evoked response magnitude (right; *-100 ms*: p = 3.2e-5, ON = 14.2 ± 0.98 Hz; OFF = 15.5 ± 1.04 Hz; *-20 ms*: p = 1.4e-6, ON = 11.8 ± 1.08 Hz, OFF = 13.9 ± 1 Hz; *+8 ms*: p = 0.0034, ON = 13.03 ± 1.03, OFF = 13.7 ± 1.03). **B** Suppressing feedback had no effect on spontaneous activity or tone-evoked response magnitude.

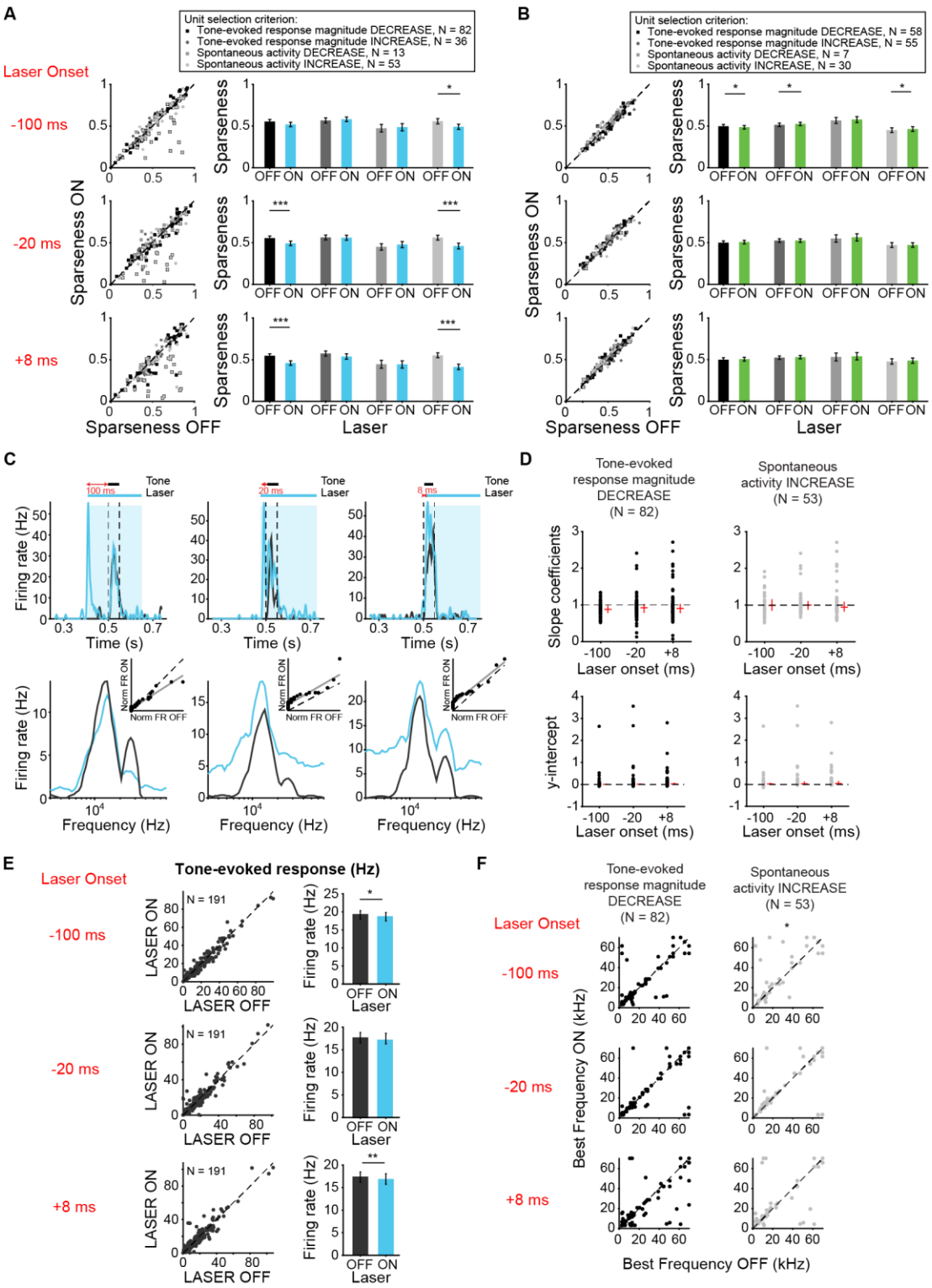

Figure 3. Effect of modulating direct cortico-collicular feedback at different latencies relative to tone onset on frequency selectivity in IC. **A** Left panels: Sparseness for laser on versus laser off trials. Right panels: Average sparseness for laser on and laser off trials. Activating feedback decreased frequency selectivity in a subset of units (mag decrease: *-20 ms*, p = 0.00031, sparse ON = 0.49 ± 0.027, sparse OFF = 0.55 ± 0.025; *+8 ms*, p = 0.00029, sparse ON = 0.46 ± 0.027, sparse OFF = 0.55 ± 0.024; spont increase: *-100 ms*, p = 0.011, sparse ON = 0.49 ± 0.032, sparse OFF = 0.56 ± 0.031; *-20 ms*, p = 0.00018, sparse ON = 0.46 ± 0.034, sparse OFF = 0.56 ± 0.029; *+8 ms*, p = 2.2e-6, sparse ON = 0.41 ± 0.032, sparse OFF = 0.55 ± 0.029). **B** Left panels: Sparseness for laser on

versus laser off trials. Right panels: Average sparseness for laser on and laser off trials. Suppressing feedback has little effect on frequency selectivity (mag decrease: -100 ms, p = 0.011, sparse ON = 0.53 ± 0.021, sparse OFF = 0.51 ± 0.021; mag increase: -100 ms, p = 0.019, sparse ON = 0.48 ± 0.021, sparse OFF = 0.49 ± 0.021; spont increase: -100 ms, p = 0.043, sparse ON = 0.46 ± 0.029, sparse OFF = 0.45 ± 0.029). **C** Example unit response timecourse (top) and tuning curves (bottom) for laser on (blue) and laser off (grey) conditions. Bottom insets represent ranked linear fits for example unit. **D** Slope coefficients (top, mag decrease: -*100 ms*, median = 0.88; -*20 ms*, median = 0.92; +*8 ms*, median = 0.903; spont increase: -*100 ms*, median = 0.99; -*20 ms*, median = 1; +*8 ms*, median = 0.94) and y-intercepts (bottom, mag decrease: -*100 ms*, median = 0.0086; -*20 ms*, median = 0.014; +*8 ms*, median = 0.022; spont increase: -*100 ms*, median = 0.014; -*20 ms*, median = 0.025; +*8 ms*, median = 0.037) of ranked linear fits, red horizontal lines indicate median, red vertical lines indicate interquartile range. E Left panels: Tone-evoked response for laser on versus laser off trials. Right panels: Average tone-evoked response for laser on and laser off trials. Activating feedback slightly decreased tone-evoked response, averaged across 7 most preferred frequencies (-*100ms*: p = 0.018, ON = 19.01 ± 1.2 Hz, OFF = 18.5 ± 1.2 Hz; +*8ms*: p = 0.007, ON = 17.3 ± 1.2 Hz; OFF = 16.9 ± 1.2 Hz) **F** Best frequencies for laser off versus laser on trials. Activating feedback had little effect on best frequency (spont increase: -*100 ms*, p = 0.022).

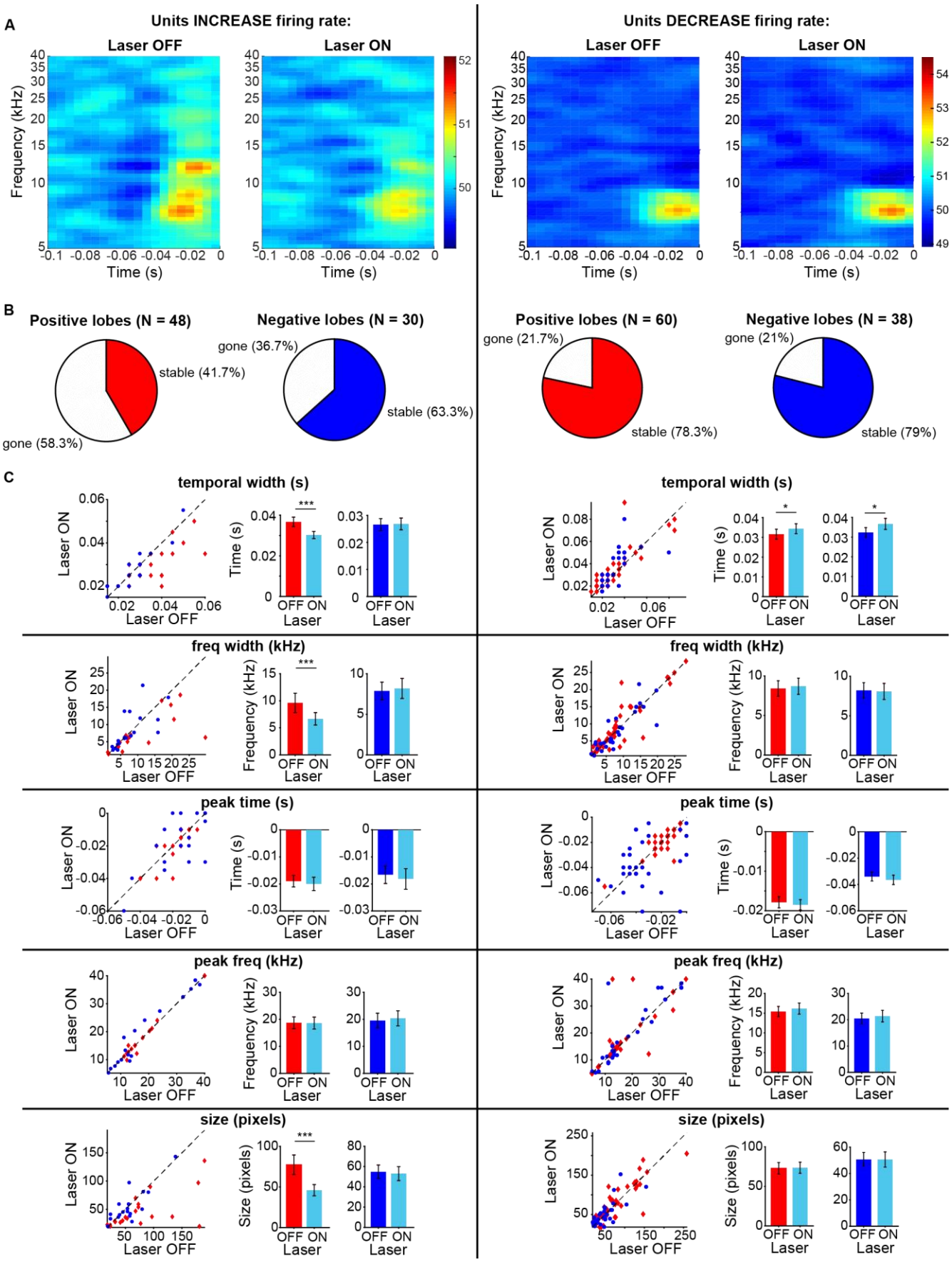
A
Units INCREASE firing rate:
Laser OFF
Laser ON
Units DECREASE firing rate:
Frequency (kHz)
Time (s)
B
Positive lobes (N = 48)
Negative lobes (N = 30)
Positive lobes (N = 60)
Negative lobes (N = 38)
gone (36.7%)
stable (41.7%)
stable (63.3%)
gone (58.3%)
gone (21.7%)
stable (78.3%)
gone (21%)
stable (79%)
C
temporal width (s)
freq width (kHz)
peak time (s)
peak freq (kHz)
size (pixels)
Laser ON
Laser OFF
Time (s)
Frequency (kHz)
Size (pixels)
OFF ON
Laser

Figure 4. Effects of activating direct cortico-collicular feedback on STRF properties. **A** Example STRF with and without activation of feedback for units that increase firing rate (left) and decrease firing rate (right) in response to feedback activation. **B** Number of positive and negative lobes that persisted with laser (stable). **C** Changes in STRF parameters of stable positive and negative lobes. Left panels: STRF parameter for laser off versus laser on trials. Center panels: Average positive lobe STRF parameter for laser on and laser off trials. Right panels: Average negative lobe STRF parameter for laser on and laser off trials. For units with an increase in firing rate we observed a decrease in temporal width ($p = 0.00098$, ON = 0.0303 ± 0.0018 s, OFF = 0.037 ± 0.0023 s), frequency width ($p = 0.00042$, ON = 6.7 ± 1.1 Hz, OFF = 9.6 ± 1.8 Hz), and overall size ($p = 0.00036$, ON = 46.05 ± 6.9 pixels, OFF = 77.5 ± 12.04 pixels) of positive lobes. For units with a decrease in firing rate we observed only a small increase in temporal width for both positive ($p = 0.026$, ON = 0.034 ±0.0025 s, OFF = 0.032 ± 0.0025 s) and negative ($p = 0.02$, ON = 0.037 ± 0.0028 s, OFF = 0.032 ± 0.0024 s) lobes.

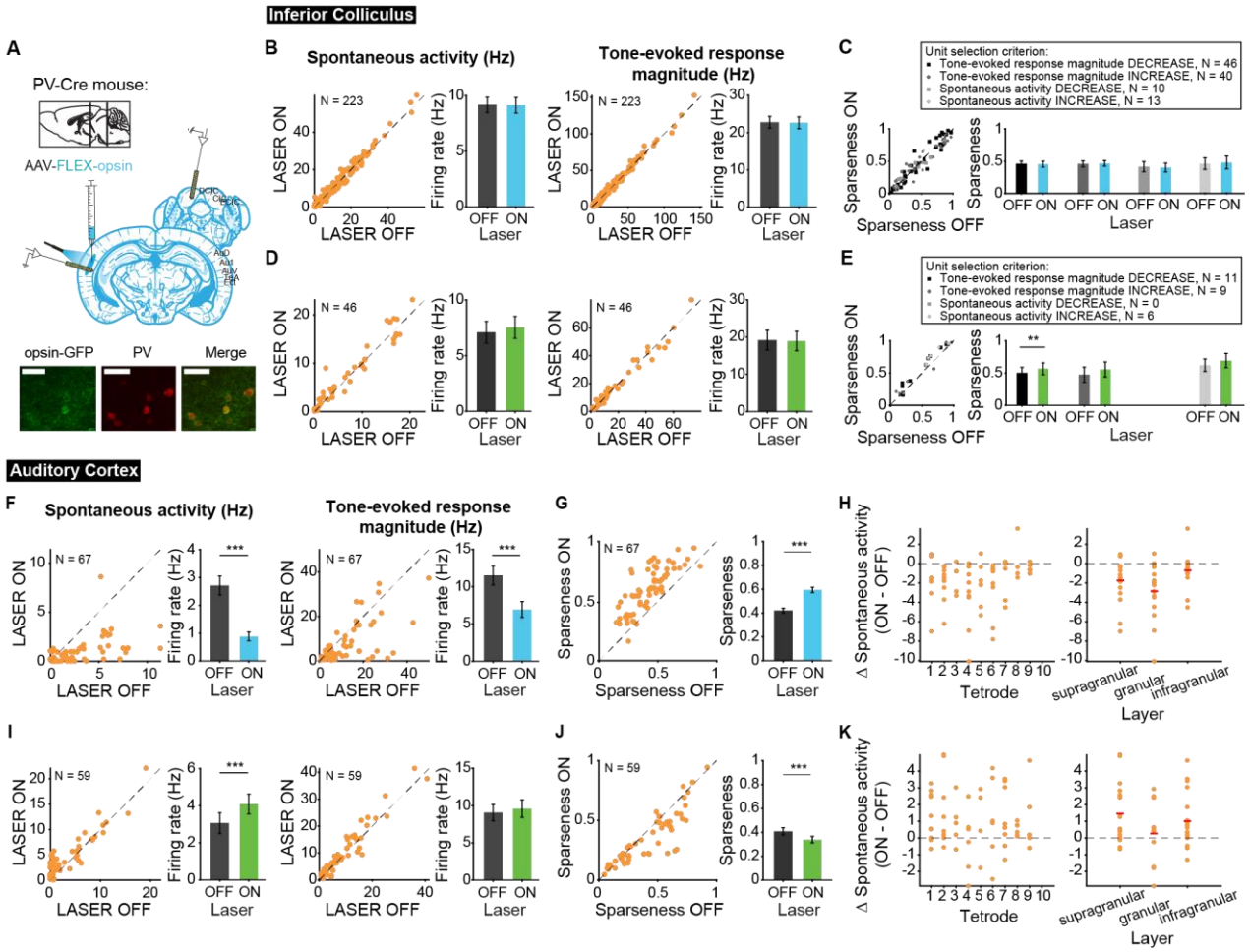

Figure 5. Effects of modulating PV interneurons in AC on tone-evoked responses in IC. **A** Stain for PV (center) and opsin-GFP (left). Scale bar: 50um. **B** Activating PVs had no effect on spontaneous activity or tone-evoked response magnitude in IC. **C** Activating PVs had no effect on frequency selectivity in IC. **D** Suppressing PVs had no effect on spontaneous activity or tone-evoked response magnitude in IC. **E** Suppressing PVs had weak effects on frequency selectivity in IC (mag decrease: p = 0.0068, ON = 0.57 ± 0.092, OFF = 0.5 ± 0.087). **F** Activating PVs decreased spontaneous activity (p = 2.2e-9, ON = 0.88 ± 0.16 Hz, OFF = 2.7 ± 0.34 Hz) and tone-evoked response magnitude (p = 8.02e-7, ON = 6.9 ± 1.06 Hz, OFF = 11.5 ± 1.3 Hz) in AC. **G** Activating PVs increased frequency selectivity in putative excitatory units in AC (p = 3.3e-12, ON = 0.59 ± 0.022, OFF = 0.42 ± 0.02). **H** Activating PVs affected putative excitatory units across all layers of AC. **I** Suppressing PVs increased spontaneous activity (p = 5.2e-5, ON = 4.08 ± 0.54 Hz, OFF = 3.06 ± 0.55 Hz) but does not affect tone-evoked response magnitude in AC. **J** Suppressing PVs decreased frequency selectivity in AC (p = 3.8e-5, ON = 0.34 ± 0.027, OFF = 0.41 ± 0.031). **K** Suppressing PVs affected putative excitatory units across all layers of AC. **B,D,F,I** Left panels: neuronal activity (spontaneous, left or tone-evoked, right) on laser on versus laser off trials. Right panels: Average neuronal activity (spontaneous, left or tone-evoked, right) for laser on and laser off trials. **C,E,G,J** Left panels: Sparseness for laser on versus laser off trials. Right panels: Average sparseness for laser on and laser off trials. **H,K** Change in spontaneous activity (laser on trials – laser off trials), left panels: for units at

each tetrode; right panels: separated into supragranular: tetrodes 1-3; granular: tetrodes 5,6; infragranular: tetrodes 7-10.

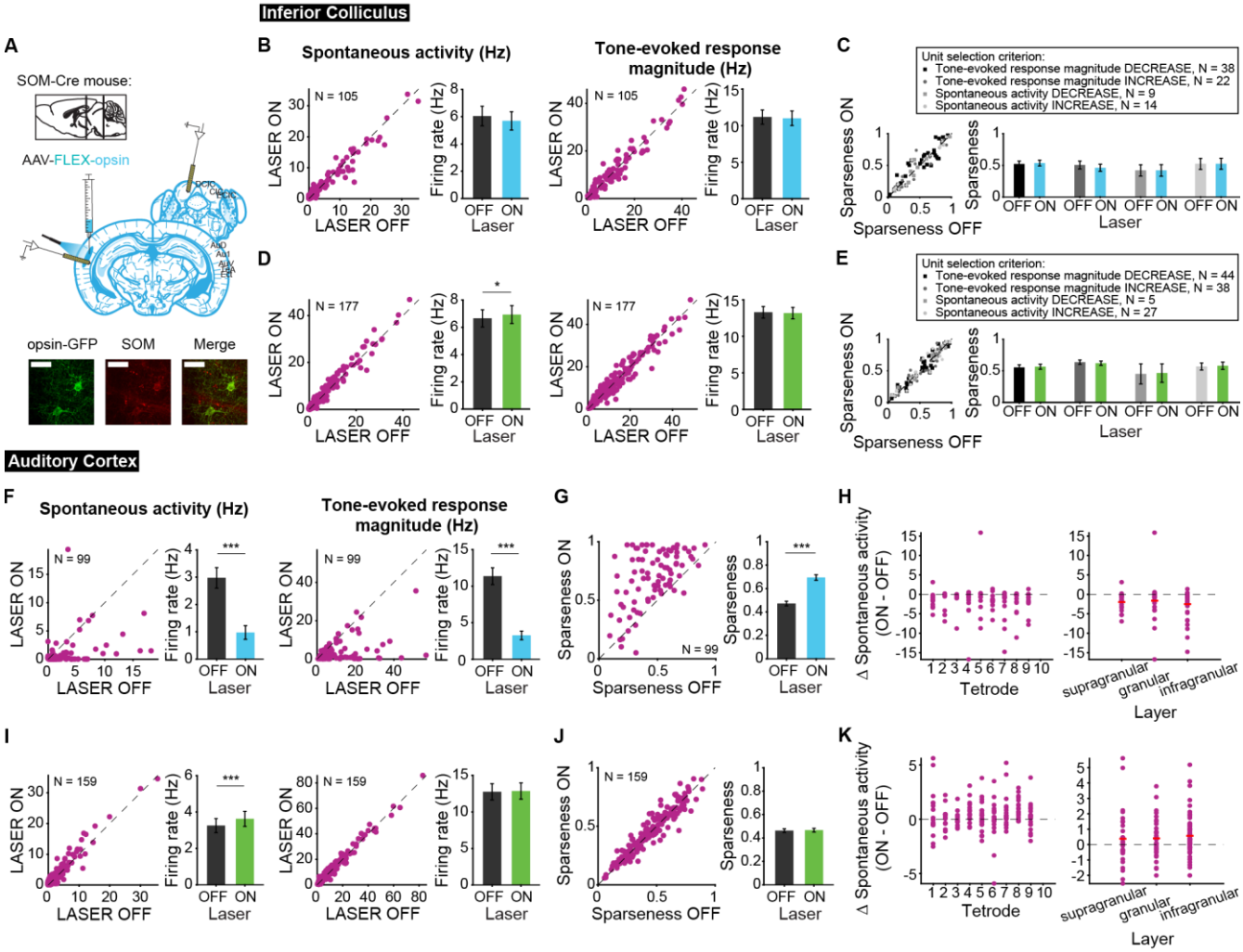

Figure 6. Effects of modulating SOM interneurons in AC on tone-evoked responses in IC. **A** Stain for SOM (center) and opsin-GFP (left). Scale bar: 50um. **B** Activating SOMs had no effect on spontaneous activity or tone-evoked response magnitude in IC. **C** Activating SOMs had no effect on frequency selectivity in IC. **D** Suppressing SOMs increased spontaneous activity (p = 0.029, ON = 6.9 ± 0.66 Hz, OFF = 6.7 ± 0.63 Hz) but did not affect tone-evoked response magnitude in IC. **E** Suppressing SOMs had no effect on frequency selectivity in IC. **F** Activating SOMs decreased spontaneous activity (p = 1.4e-12, ON = 0.97 ± 0.25 Hz, OFF = 2.9 ± 0.37 Hz) and tone-evoked response magnitude (p = 1.3e-15, ON = 3.3 ± 0.59 Hz, OFF = 11.4 ± 1.2 Hz) in AC. **G** Activating SOMs increased frequency selectivity in putative excitatory units in AC (p = 1.6e-13, ON = 0.69 ± 0.024, OFF = 0.47 ± 0.019). **H** Activating SOMs affected putative excitatory units across all layers of AC. **I** Suppressing SOMs increased spontaneous activity (p = 8.1e-4, ON = 3.6 ± 0.41 Hz, OFF = 2.2 ± 0.38 Hz) but did not affect tone-evoked response magnitude in AC. **J** Suppressing SOMs had no effect on frequency selectivity in AC. **K** Suppressing SOMs affected putative excitatory units across all layers of AC. **B,D,F,I** Left panels: neuronal

activity (spontaneous, left or tone-evoked, right) on laser on versus laser off trials. Right panels: Average neuronal activity (spontaneous, left or tone-evoked, right) for laser on and laser off trials. **C,E,G,J** Left panels: Sparseness for laser on versus laser off trials. Right panels: Average sparseness for laser on and laser off trials. **H,K** Change in spontaneous activity (laser on trials – laser off trials), left panels: for units at each tetrode; right panels: separated into supragranular: tetrodes 1-3; granular: tetrodes 5,6; infragranular: tetrodes 7-10.

References

Aizenberg M, Geffen MN (2013) Bidirectional effects of aversive learning on perceptual acuity are mediated by the sensory cortex. Nat Neurosci 16:994–996.

Aizenberg M, Mwilambwe-Tshilobo L, Briguglio JJ, Natan RG, Geffen MN (2015) Bidirectional Regulation of Innate and Learned Behaviors That Rely on Frequency Discrimination by Cortical Inhibitory Neurons. PLoS Biol 13:1–32.

Alitto HJ, Usrey WM (2003) Corticothalamic feedback and sensory processing. Curr Opin Neurobiol 13:440–445.

Bajo VM, Moore DR (2005) Descending projections from the auditory cortex to the inferior colliculus in the gerbil, Meriones unguiculatus. J Comp Neurol 486:101–116.

Bajo VM, Nodal FR, Bizley JK, Moore DR, King a. J (2006) The Ferret Auditory Cortex: Descending Projections to the Inferior Colliculus. Cereb Cortex 17:475–491.

Bajo VM, Nodal FR, Moore DR, King AJ (2009) The descending corticocollicular pathway mediates learning-induced auditory plasticity. Nat Neurosci 13:253–260.

Barnstedt O, Keating P, Weissenberger Y, King AJ, Dahmen JC (2015) Functional Microarchitecture of the Mouse Dorsal Inferior Colliculus Revealed through In Vivo Two-Photon Calcium Imaging. J Neurosci 35:10927–10939.

Carruthers IM, Natan RG, Geffen MN (2013) Encoding of ultrasonic vocalizations in the auditory cortex. J Neurophysiol 109:1912–1927.

Chauvin A, Worsley KJ, Schyns PG, Arguin M, Gosselin F (2005) Accurate statistical tests for smooth classification images. J Vis 5:659–667.

Coomes DL, Schofield RM, Schofield BR (2005) Unilateral and bilateral projections from cortical cells to the inferior colliculus in guinea pigs. Brain Res 1042:62–72.

Doucet JR, Molavi DL, Ryugo DK (2003) The source of corticocollicular and corticobulbar projections in area Te1 of the rat. Exp Brain Res 153:461–466.

Downer JD, Rapone B, Verhein J, O'Connor KN, Sutter ML (2017) Feature-Selective Attention Adaptively Shifts Noise Correlations in Primary Auditory Cortex. J Neurosci 37:5378–5392.

Ehret G, Egorova M, Hage SR, Müller BA (2003) Spatial map of frequency tuning-curve shapes in the mouse inferior colliculus. Neuroreport 14:1365–1369.

Feliciano M, Potashner SJ (1995) Evidence for a Glutamatergic Pathway from the Guinea Pig Auditory Cortex to the Inferior Colliculus. J Neurochem 65:1348–1357.

Fendt M, Li L, Yeomans JS (2001) Brain stem circuits mediating prepusle inhibition of the startle reflex. Psychopharmacology (Berl) 156:216–224.

Fritz J, Shamma S, Elhilali M, Klein D (2003) Rapid task-related plasticity of spectrotemporal receptive fields in primary auditory cortex. Nat Neurosci 6:1216–1223.

Gao E, Suga N (1998) Experience-dependent corticofugal adjustment of midbrain frequency map in bat auditory system. PNAS 95:12663–12670.

Gao E, Suga N (2000) Experience-dependent plasticity in the auditory cortex and the inferior colliculus of bats : Role of the corticofugal system. PNAS 97:8081–8086.

Hamilton LS, Sohl-Dickstein J, Huth AG, Carels VM, Deisseroth K, Bao S (2013) Optogenetic activation of an inhibitory network enhances feedforward functional connectivity in auditory cortex. Neuron 80:1066–1076.

Jen PH-S, Chen QC, Sun XD (1998) Corticofugal regulation of auditory sensitivity in the bat inferior colliculus. J Comp Physiol A 183:683–697.

Jen PH-S, Zhou X (2003) Corticofugal modulation of amplitude domain processing in the midbrain of the big brown bat, Eptesicus fuscus. Hear Res 184:91–106.

Lakatos P, Musacchia G, O'Connel MN, Falchier AY, Javitt DC, Schroeder CE (2013) The spectrotemporal filter mechanism of auditory selective attention. Neuron 77:750–761.

Leitner DS, Cohen ME (1985) Role of the inferior colliculus in the inhibition of acoustic startle in the rat. Physiol Behav 34:65–70.

Li L, Frost BJ (2000) Azimuthal directional sensitivity of prepulse inhibition of the pinna startle reflex in decerebrate rats. Brain Res Bull 51:95–100.

Li L, Korngut LM, Frost BJ, Beninger RJ (1998) Prepulse inhibition following lesions of the inferior colliculus: prepulse intensity functions. Physiol Behav 65:133–139.

Li L, Yue Q (2002) Auditory gating processes and binaural inhibition in the inferior colliculus. Hear Res 168:98–109.

Lim HH, Anderson DJ (2007) Antidromic Activation Reveals Tonotopically Organized Projections From Primary Auditory Cortex to the Central Nucleus of the Inferior Colliculus in Guinea Pig. J Neurophysiol 97:1413–1427.

Ma X, Suga N (2001a) Plasticity of Bat's Central Auditory System Evoked by Focal Electric Stimulation of Auditory and/or Somatosensory Cortices. J Neurophysiol 85:1078–1087.

Ma X, Suga N (2001b) Corticofugal modulation of duration-tuned neurons in the midbrain auditory nucleus in

bats. PNAS 98:14060–14065.

Malmierca MS, Izquierdo MA, Cristaudo S, Hernandez O, Perez-Gonzalez D, Covey E, Oliver DL (2008) A Discontinuous Tonotopic Organization in the Inferior Colliculus of the Rat. J Neurosci 28:4767–4776.

Malmierca MS, Rees A, Le Beau FEN, Bjaalie JG (1995) Laminar organization of frequency-defined local axons within and between the inferior colliculi of the guinea pig. J Comp Neurol 357:124–144.

Markovitz CD, Tang TT, Lim HH (2013) Tonotopic and localized pathways from primary auditory cortex to the central nucleus of the inferior colliculus. Front Neural Circuits 7:1–11.

McGinley MJ, David S V, McCormick DA (2015) Cortical Membrane Potential Signature of Optimal States for Sensory Signal Detection. Neuron 87:179–192.

Miller KE, Casseday JH, Covey E (2005) Relation between intrinsic connections and isofrequency contours in the inferior colliculus of the big brown bat, Eptesicus fuscus. Neuroscience 136:895–905.

Natan RG, Carruthers IM, Mwilambwe-Tshilobo L, Geffen MN (2017a) Gain Control in the Auditory Cortex Evoked by Changing Temporal Correlation of Sounds. Cereb cortex 27:2385–2402.

Natan RG, Rao W, Geffen MN (2017b) Cortical Interneurons Differentially Shape Frequency Tuning following Adaptation. Cell Rep 21:878–890.

Phillips EA, Hasenstaub AR (2016) Asymmetric effects of activating and inactivating cortical interneurons. Elife 5:1–22.

Popelář J, Nwabueze-Ogbo FC, Syka J (2003) Changes in Neuronal Activity of the Inferior Colliculus in Rat after Temporal Inactivation of the Auditory Cortex. Physiol Res 52:615–628.

Popelář J, Šuta D, Lindovský J, Bureš Z, Pysanenko K, Chumak T, Syka J (2016) Cooling of the auditory cortex modifies neuronal activity in the inferior colliculus in rats. Hear Res 332:7–16.

Rouiller EM, Durif C (2004) The dual pattern of corticothalamic projection of the primary auditory cortex in macaque monkey. Neurosci Lett 358:49–52.

Rudy B, Fishell G, Lee S, Hjerling-Leffler J (2011) Three groups of interneurons account for nearly 100% of neocortical GABAergic neurons. Dev Neurobiol 71:45–61.

Saldaña E, Feliciano M, Mugnaini E (1996) Distribution of descending projections from primary auditory neocortex to inferior colliculus mimics the topography of intracollicular projections. J Comp Neurol 371:15–40.

Saldaña E, Merchań MA (1992) Intrinsic and commissural connections of the rat inferior colliculus. J Comp Neurol 319:417–437.

Schneider DM, Woolley SMN (2010) Discrimination of Communication Vocalizations by Single Neurons and Groups of Neurons in the Auditory Midbrain. J Neurophysiol 103:3248–3265.

Schofield BR, Motts SD (2009) Projections from auditory cortex to cholinergic cells in the midbrain tegmentum of guinea pigs. Brain Res Bull 80:163–170.

Seybold BA, Elizabeth AK, Schreiner CE, Hasenstaub AR, Seybold BA, Phillips EAK, Schreiner CE,

Hasenstaub AR (2015) Inhibitory Actions Unified by Network Integration Viewpoint Inhibitory Actions Unified by Network Integration. Neuron 87:1181–1192.

Shechter B, Depireux DA (2007) Stability of spectro-temporal tuning over several seconds in primary auditory cortex of the awake ferret. Neuroscience 148:806–814.

Straka MM, Hughes R, Lee P, Lim HH (2015) Descending and tonotopic projection patterns from the auditory cortex to the inferior colliculus. Neuroscience 300:325–337.

Sturm J, Nguyen T, Kandler K (2014) Development of intrinsic connectivity in the central nucleus of the mouse inferior colliculus. J Neurosci 34:15032–15046.

Syka J, Popelář J, Kvašňák E, Astl J (2000) Response properties of neurons in the central nucleus and external and dorsal cortices of the inferior colliculus in guinea pig. Exp Brain Res 133:254–266.

Vila C-H, Williamson RS, Hancock KE, Polley DB (2019) Optimizing optogenetic stimulation protocols in auditory corticofugal neurons based on closed-loop spike feedback. bioRxiv.

Weliky M, Fiser J, Hunt RH, Wagner DN (2003) Coding of Natural Scenes in Primary Visual Cortex. Neuron 37:703–718.

Winer JA, Diehl JJ, Larue DT (2001) Projections of auditory cortex to the medial geniculate body of the cat. J Comp Neurol 430:27–55.

Winer JA, Larue DT, Diehl JJ, Hefti BJ (1998) Auditory cortical projections to the cat inferior colliculus. J Comp Neurol 400:147–174.

Wood KC, Blackwell JM, Geffen MN (2017) Cortical inhibitory interneurons control sensory processing. Curr Opin Neurobiol 46:200–207.

Woolley SMN, Gill PR, Theunissen FE (2006) Stimulus-Dependent Auditory Tuning Results in Synchronous Population Coding of Vocalizations in the Songbird Midbrain. J Neurosci 26:2499–2512.

Xiong XR, Liang F, Zingg B, Ji X, Ibrahim LA, Tao HW, Zhang LI (2015) Auditory cortex controls sound-driven innate defense behaviour through corticofugal projections to inferior colliculus. Nat Commun 6:7224.

Yan J, Zhang Y, Ehret G, Yan J (2005) Corticofugal shaping of frequency tuning curves in the central nucleus of the inferior colliculus of mice. J Neurophysiol 93:71–83.

Yan W, Suga N (1998) Corticofugal modulation of the midbrain frequency map in the bat. Nat Neurosci 1:54–58.

Zhang Y, Suga N, Yan J (1997) Corticofugal modulation of frequency processing in bat auditory system. Nature 387:900–903.

Zhou X, Jen PH-S (2005) Corticofugal modulation of directional sensitivity in the midbrain of the big brown bat, Eptesicus fuscus. Hear Res 203:201–215.

Zhou X, Jen PH-S (2007) Corticofugal Modulation of Multi-Parametric Auditory Selectivity in the Midbrain of the Big Brown Bat. J Neurophysiol 98:2509–2516.